This is the Pre-Published Version.
S. Wang, Y. Zhang, X. Huang (2021) *Ignition of EPS Foam by a Hollow Particle: Threshold, Auto-ignition, and Fire Point*, **Combustion and Flame**, 232, 111524 https://doi.org/10.1016/j.combustflame.2021.111524

Ignition of EPS Foam by a Hot Moving Hollow Particle: Threshold, Auto-ignition, and Fire Point

Supan Wang [a, b], Yu Zhang [a], Xinyan Huang [b, *]

[a] *College of Safety Science and Engineering, Nanjing Tech University, Nanjing, Jiangsu 210009, China*

[b] *Research Centre for Fire Safety Engineering, Department of Building Services Engineering, The Hong Kong Polytechnic University, Kowloon, Hong Kong.*

*Corresponding to xy.huang@polyu.edu.hk

Abstract:

The ignition of building insulation materials by hot moving inert particles from fireworks display and welding processes is responsible for many tragic building fires. In this work, a hot hollow steel particle with various void ratio and diameter is dropped to ignite the low-density (16 kg/m^3) expandable polystyrene (EPS) foam with three back boundary conditions. Results show that the minimum ignition temperature of hollow particles is close to solid particles (about 800 °C), and the temperature and size of particle are better measures of the spotting fire hazard than the particle mass and energy. As the void ratio increases, the minimum particle temperature for ignition first slightly decreases because the residence time of moving particle increases. For extremely hollow particles, ignition requires a much higher particle temperature to overcome the fast cooling. Besides the piloted ignition by hot particle, the auto-ignition phenomenon is observed for the first time, which is controlled by time scales of mixing and cooling. Moreover, the semi-open fuel back boundary shows the biggest fire hazard, because both good oxygen supply and long particle residence time promote the ignition to the fire point and fuel burnout. This study deepens the understanding of the complex interaction between hot porous particles and foam materials in the spotting ignition process of the building façade.

Keywords: *Ignition limit; Insulation materials; Façade fire; Porous particles; Spotting fire.*

1. Introduction

With the rapid social-economic development and urbanization, the number of skyscrapers and high-rise buildings is increasing at an unprecedented speed. To improve the building energy efficiency, many high-molecular organic polymers with low thermal conductivity are widely used as building thermal insulation and facade, such as expanded polystyrene (EPS) foam and polyurethane (PU) foam [1,2]. Thus, the fire hazard of these flammable materials is still a primary safety concern [3–6], and these materials can be ignited by hot metal particles generated from the fireworks display (Fig. 1a), electrical faults [7], machining, and welding processes [8] (Fig. 1b) to cause disastrous fires. For example, the Beijing TVCC fire (2009) was ignited by metal particles from a firework show (Fig. 1c) [9]. Both the

Shanghai high-rise residential hall fire (2010) and the New Zealand International Convention Centre Fire (2019) were ignited by hot metal particles from welding work [10]. Therefore, understanding the process and risk of hot-particle ignition of building insulation materials is of great importance for the building fire safety [11–14].

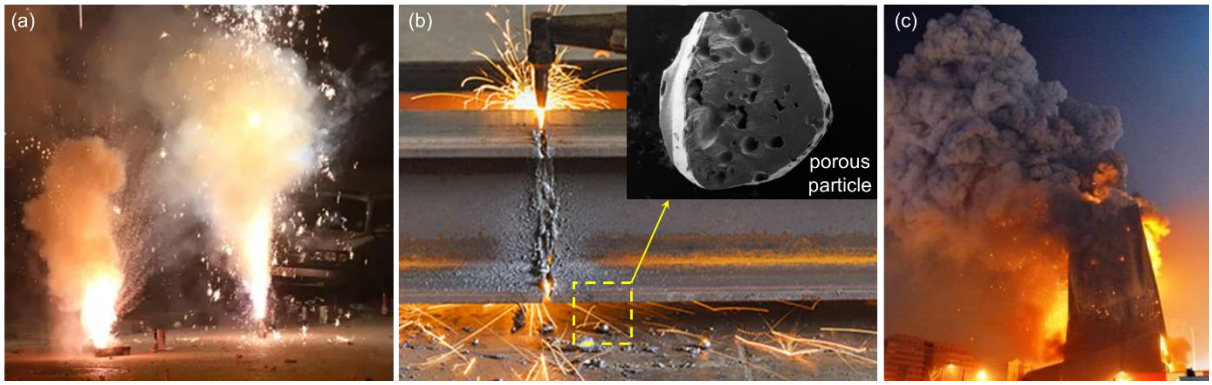

Fig. 1. Hot metal particles produced from (a) the fireworks display, (b) the formation and porous structure of a welding particle, and (c) the 2009 façade fire on Beijing TVCC building ignited by firework particles.

The process of hot-particle ignition is fundamentally different from the common flame ignition or the radiation-driven ignition [11–19]. It is because the hot particle is not only the heat source to heat the solid fuel, but also the pilot source to ignite the pyrolysis gases [11,20]. The hot particle can also induce smoldering that may transition to a flame [21,22]. The propensity of hot-particle ignition depends on the particle (temperature, size, energy, material, etc.) [8,22–26], the interaction with the fuel bed [13,27], the fuel bed properties (density, moisture, composition, etc.) [13,26–28] and the environment (humidity, wind, etc.) [27,29]. Some natural particles are reactive (e.g., firebrands and embers), and their ignition processes are more complex than inert particles, as revealed in [11,30–36].

Previous work showed that for a large hot metal particle (> 8 mm), a minimum temperature of about 800 °C was needed to ignite the EPS foam, while the sample density and thickness had a small influence [13,37]. Compared to temperature, the metal type (various thermal properties) played a weak role in the ignition, unless the metal like copper and some alloys melt [15,23]. For tiny particles (< 8 mm), the required particle temperature for ignition quickly increased with decreasing size [15,23], because of both small energy and fast cooling. All these previous studies focused on solid particles. However, real metal particles in practice could be hollow and highly porous (Fig. 1b). Thus, the thermal energy of a larger porous particle could be smaller than that of a small solid particle, which questions *whether the size or energy of the particle is a good measure of its spotting fire hazard*.

The ignition of plastic foam by hot metal particles was controlled by the competition between the gas mixing time and the particle residence time [13]. When the hot flying particles often have a large velocity, they may not stay in contact with the fuel bed, but bounce away or embed into the fuel; that is, they only have a short contact time with the foam. Moreover, for a particle that is hot enough to pilot a flame, it can also quickly melt and embed into the plastic foam. Thus, the ignition process of the hot

moving particle is significantly affected by contact between fuel and particle, as well as the oxygen supply. On the other hand, the fast-moving small metal particle can be quickly cooled due to a large convection coefficient and curvature effect. Inert particles are different from embers because embers may trigger a stronger smoldering process in the wind. So far, *the overall effects of moving particle residence conditions and oxygen supply on spotting ignition are still not well understood*, posing a big knowledge gap.

In this work, we investigate the spotting ignition of EPS foam by hollow steel particles. The particle energy changes with the size, temperature, and void ratio. The oxygen supply is changed by the fuel-bed back boundary. Various hot-particle ignition phenomena are observed and described in detail. Then, the ignition limit, relating to the temperature, diameter, mass, energy, and void ratio of the particle, is quantified. Afterward, the hot-particle ignition mechanism of insulation materials is analyzed using heat and mass transport theories.

2. Experimental methods

2.1. Apparatus

The experimental setup of hot particle ignition, upgraded from our previous work [13,27], is illustrated in Fig. 2. It mainly consisted of a tubular furnace (SK 2-2.5-13 TS, 0~2.5 kW) to heat the metal particle, the heating power control system to regulate the furnace temperature, and the sample holder unit to support the sample. The furnace was heated by silicon carbide heating elements to a preset temperature (800-1300 ºC) and regulated by a Type-S thermocouple and the control system.

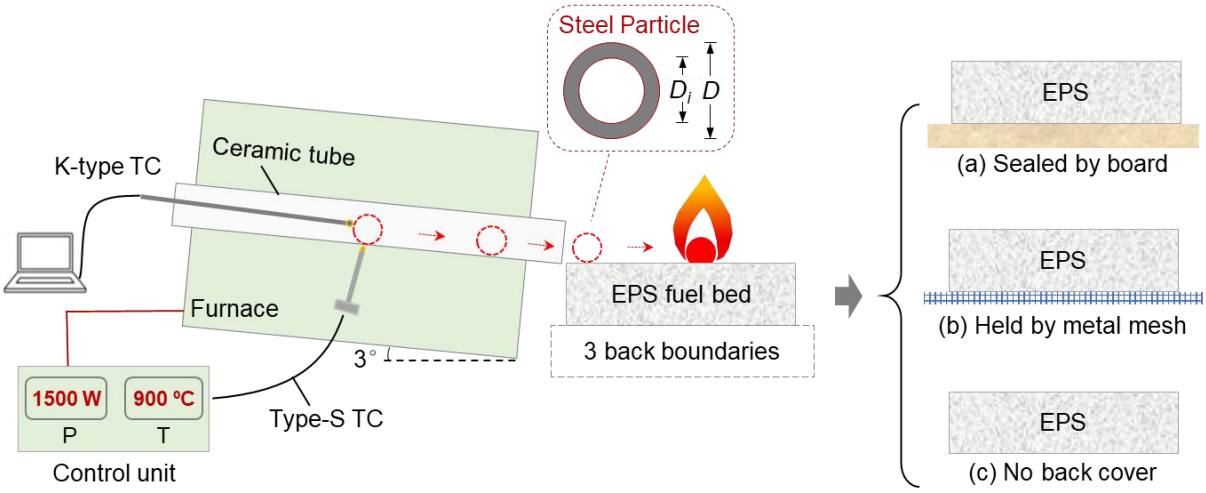

Fig. 2. Schematic of the experimental setup for hot particle ignition of EPS foam. The hot particle is a thin-walled hollow particle with an inner (D_i) and outer (D) diameter. And EPS Fuel bed was supported by three characteristic boundary conditions.

2.2. Hot hollow steel particles

Spherical steel particles of the various void ratio and diameter were tested, which mimicked the porous metal particles in real firework and welding processes. These hollow steel particles were

specially made by welding two steel shell hemispheres that have different wall thicknesses. The void ratio (e) or the overall porosity can be defined as

$$e = 1 - \frac{m}{m_s} = 1 - \frac{\rho V}{\rho_s V} = \left(\frac{D_i}{D}\right)^3 \quad (1)$$

where m is the particle mass, m_s is the mass of the solid particle; V is the particle volume; ρ is the apparent particle density, and ρ_s is the material density of the steel; D_i and D are the inner and outer diameter of the particle (see Fig. 2). For solid particles, $e = 0$. Because the machining process for these hollow particles was challenging, the void ratio (e) could not be made the same for particles of all sizes. The mass of the particle (m or m_s) was measured before the experiment. The calculated void ratios (e) and inner diameters (D_i) of four diameters (D) are listed in Table 1.

Table 1. Size and void ratio of the hot particle in the experiment, where '-' means the particles with higher void ratios are not available in the market.

***D* = 8 mm**				***D* = 10 mm**				***D* = 12 mm**				***D* = 16 mm**			
e	***Di***	***m***	***ρ***	***e***	***Di***	***m***	***ρ***	***e***	***Di***	***m***	***ρ***	***e***	***Di***	***m***	***ρ***
(-)	**(mm)**	**(g)**	**(g/cm³)**	**(-)**	**(mm)**	**(g)**	**(g/cm³)**	**(-)**	**(mm)**	**(g)**	**(g/cm³)**	**(-)**	**(mm)**	**(g)**	**(g/cm³)**
0.00	0.0	2.1	8.0	0.00	0.0	4.2	8.0	0.00	0.0	7.2	8.0	0.00	0.0	16.6	8.0
0.57	6.6	0.9	3.3	0.72	9.0	1.2	2.3	0.59	10.0	3.0	3.3	0.73	14.4	4.5	2.1
-	-			-	-			0.68	10.5	2.3	2.5	0.80	14.8	3.4	1.6
-	-			-	-			-	-			0.85	15.1	2.5	1.2

2.3. EPS Fuel bed

Based on our previous research, the non-retardant EPS foams were chosen as the typical building insulation material. EPS was catalyzed and polymerized by styrene. The element analysis of the EPS foam showed 91.6, 7.7, 1.4, 0.5% mass fractions for C, H, O, N, respectively. The thermal analysis showed that the pyrolysis temperature of this EPS sample was about 250-300 °C (see Appendix). The density of the fuel bed was 16 ± 0.2 kg/m³, and the sample size was cut into small samples of a 200 mm × 200 mm cross-section and 50-mm thickness. The EPS foam had a close-cell porous structure, and all side surfaces were directly exposed to ambient without the cover.

The EPS foam sample was supported by the tripod. To explore the oxygen supply conditions on the hot particle ignition and subsequent combustion process of the fuel bed, three characteristic boundary conditions (see Fig. 2) were selected as follows:

(a) Fully enclosed boundary (sealed by the fireproof board): the back of the fuel bed was physically supported by a fireproof board that prohibits the oxygen supply.

(b) Semi-open boundary (held by metal mesh): the back of the fuel bed was physically supported by mesh wire cloth, which allowed a good oxygen supply.

(c) Fully open boundary (no back cover): the back of the fuel bed was not physically supported with a free oxygen supply.

2.4. Procedures and measurements

During the ignition experiment, once the furnace temperature was stable, the particle was inserted into the center of the tubular furnace. The surface temperature of the particle was quickly increased and stabilized at a high temperature (T_p), and its temperature was recorded and calibrated by a 0.5-mm thermocouple. Once reached a steady uniform temperature, the particle was released along the inclined ceramic tube. The end of the ceramic tube was rested on the surface of the fuel bed to minimize the impact and bounce of the particle.

The motion and ignition processes of the hot particle were recorded with two video cameras (at 50 frames per second) from a front view and a 45º bird's-eye view. Because of the complexity and randomness in experimental conditions, at least 5-6 repeated runs were conducted for each set of experimental conditions to quantify the probability of each experimental outcome.

3. Experimental results

Depending on the particle temperature and its interaction with the fuel bed, both a short-term flame (i.e., ignition point) and a long-lasting flame that burnt out the fuel (i.e., the fire point) were observed. The smoldering ignition was never observed because the pyrolysis of EPS produced very little char.

Herein, we defined a successful flaming ignition as the presence of a visible flame that can be sustained longer than 1 s. The outcome of each test was categorized as "ignition" or "no ignition". Based on the previous work [13,27], the ignition probability (P_{ig}) was defined as the ratio of successful ignition (N_{ig}) to the repetition number (N_{tot}) as

$$P_{ig} = \frac{N_{ig}}{N_{tot}} \times 100\% \quad (2)$$

Then, we chose the temperature at 50% ignition probability as critical ignition temperature (T_{cr}), and 5-95% ignition probability as the possible ignition zone [13,22,23,27,37].

3.1. Flaming ignition phenomena

The flaming ignition of EPS foam by a rolling hot particle could occur during the particle's rolling process (i.e., *rolling ignition*) or its embedding process into the EPS foam (i.e., *embedded ignition*). Fig. 3 illustrates (a-b) typical ignition and (c) no-ignition processes, where the hollow particle had a diameter of 16 mm and a void ratio of 0.85, and the back boundary was sealed. The original video recorded by the front-view camera can be found in Supplementary Videos S1-3. The moment that a particle landing on the fuel bed was set as the time zero. Once landed, the particle rolled horizontally for 2~8 cm, before it gradually sank into the fuel bed. Usually, hollow particles would roll for a longer distance than the solid particle, because they had a lower apparent density (ρ, see Table 1).

The rolling ignition requires a high particle temperature (>850 ℃) that is not only hot enough to pilot the flame, but also reduces the mixing time to match the short residence time, as first revealed in

our previous work [13]. For hollow particles, their rolling ignition phenomenon was similar to solid particles, where a small flame was attached to the rolling particle, before it was fully embedded into the foam, as illustrated in Fig. 3(a). In other words, as long as the particle is hot enough, it can trigger the rolling ignition, regardless of the void ratio. The flame first occurred at 160 ms when the particle was still rolling horizontally over the sample surface. And the small flame continued to follow the particle until the rolling ceased.

Right after the particle stopped rolling at 300 ms, a strong premixed flame surrounded the particle, and then transition to the diffusion flame at 580 ms. Then, the particle was embedded into the fuel bed, vertically passed through the fuel by gravity, and reached the bottom fireproof board at 1,660 ms. As the EPS foam quickly shrank, once heated by the hot particle, it provided little resistance to the penetration. The entire penetration process lasted for about 1 s, which had an average velocity of about 4 cm/s. At the same time, the flame weakened, and eventually extinguished at 2,860 ms. Afterward, a vertical cavity from top to bottom was created inside the tested sample, and white smokes (likely the pyrolysis gas of EPS) continued to produce, because the particle was still hot.

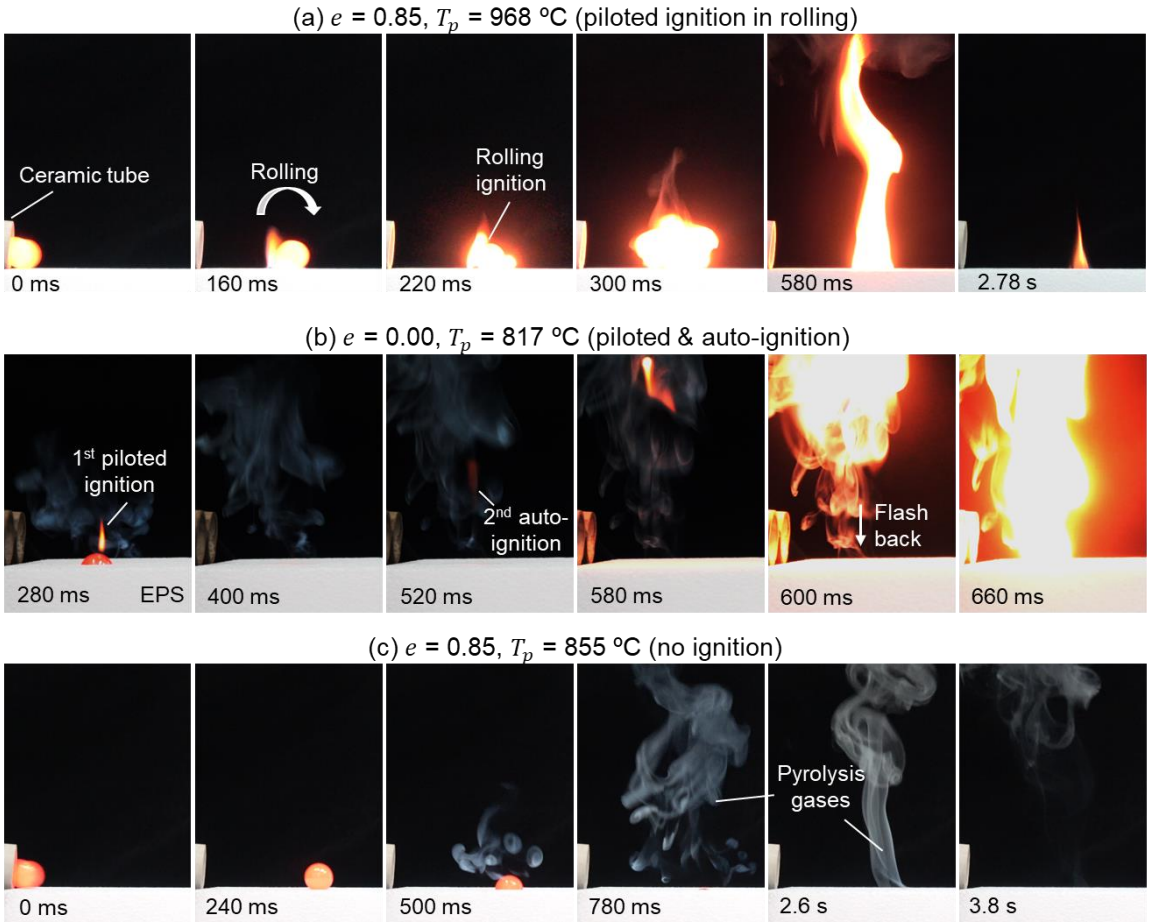

Fig. 3. Snapshot of igniting EPS foam by a solid hot particle (D = 16 mm, e = 0.85), (a) $T_p = 968$ ℃ with rolling ignition (Video S1), (b) $T_p = 817$ ℃ with two-stage piloted- and auto-ignition (Video S2), and (c) $T_p = 810$ ℃ without ignition (Video S3).

If the particle temperature was decreased to 817 ºC (Fig. 3b), a small flame (1st flash) and white smoke (*i.e.,* pyrolysis gas) occurred above the particle, right before it was fully embedded at 280 ms. The flame on the surface of the particle was quickly extinguished after about 100 ms, when the particle fully sank into the EPS foam. It is probably because there was not sufficient oxygen to maintain the flame inside the cavity. Nevertheless, the 2nd ignition occurred in the premixed pyrolysis gas and 3 cm above the fuel bed at 520 ms, which was an *auto-ignition*. Then, the flame propagated both upward to ignite the surrounding pyrolysis gas and downward to attach the fuel bed at 660 ms. This flash-back process is quite similar to the backdraft phenomena in the compartment fire [38], and it was caused by the oxygen re-supply and auto-ignition. Therefore, we can confirm that the hot-particle ignition of EPS foam involves both the piloted ignition [13] and the auto-ignition. When the particle temperature was further reduced to 810 °C (Fig. 3c), the particle was no longer hot enough to either pilot a flame or produce hot smoke for auto-ignition.

This auto-ignition only occurs in a narrow particle-temperature region, depending on the mixing of the high-temperature pyrolysis gas and air (see Fig. 4a). It is a transitional stage and easily affected by the surrounding condition. To the authors' awareness, such an auto-ignition phenomenon was not observed in any metal-particle ignition research before, due to the randomness and low probability. It is worth noting that the transitional auto-ignition occurred for most tested particles, but their critical ignition temperature and probability varied with the particle size and void ratio. More details are discussed in Section 4.3.

3.2. Ignition probability of EPS foam by hot particle

Fig. 4 presents the ignition probability of EPS foam versus the hot-particle temperature (T_p), diameter (D), mass (m), and effective energy (E). Each colored circle corresponds to more than 5 repeated runs, and the color bar scales the ignition probability from 0% (black) to 100% (white). The solid symbol presents the solid particle (including the previous data [13]), and the hollow symbol presents the hollow particle. To simplify the comparison, the critical ignition temperatures (T_{cr}) with 50% ignition probability are also replotted for solid and hollow particles in the second row. Results first showed that the measured minimum hot-particle temperature to ignite the EPS foam is about 800 °C, which is much higher than the EPS pyrolysis temperature (250-300 °C).

Note that many repeating experiments have been conducted with particles of 700 ºC and lower temperatures, but no ignition could be observed. It is because that the particle temperature is too low to pilot a flame, although sufficient EPS pyrolysis gases (smoke) have been produced. This minimum temperature is independent of the particle size, mass, and void ratio, because it is essentially the minimum temperature for the pilot source. In fact, for many other piloted ignition tests with a hot coil as the pilot source, 700 ºC is also the minimum temperature for the pilot sources [16].

Fig. 4a also demonstrates a hyperbolic relationship between particle size and temperature, with a smaller particle requiring a higher temperature to ignite the EPS foam. This trend is the same as the

previous work with solid particles [13,22,23,27]. Tiny porous particles (< 5 mm diameter) will require a much higher temperature for spotting ignition, following the hyperbolic relationship, because of the small thermal inertia and the fast cooling by the environment. Thus, larger hot particles generally pose a greater fire risk, and a larger number of tiny particles can accumulate a pile that act as the larger size particle, like the firebrand pile [39,40].

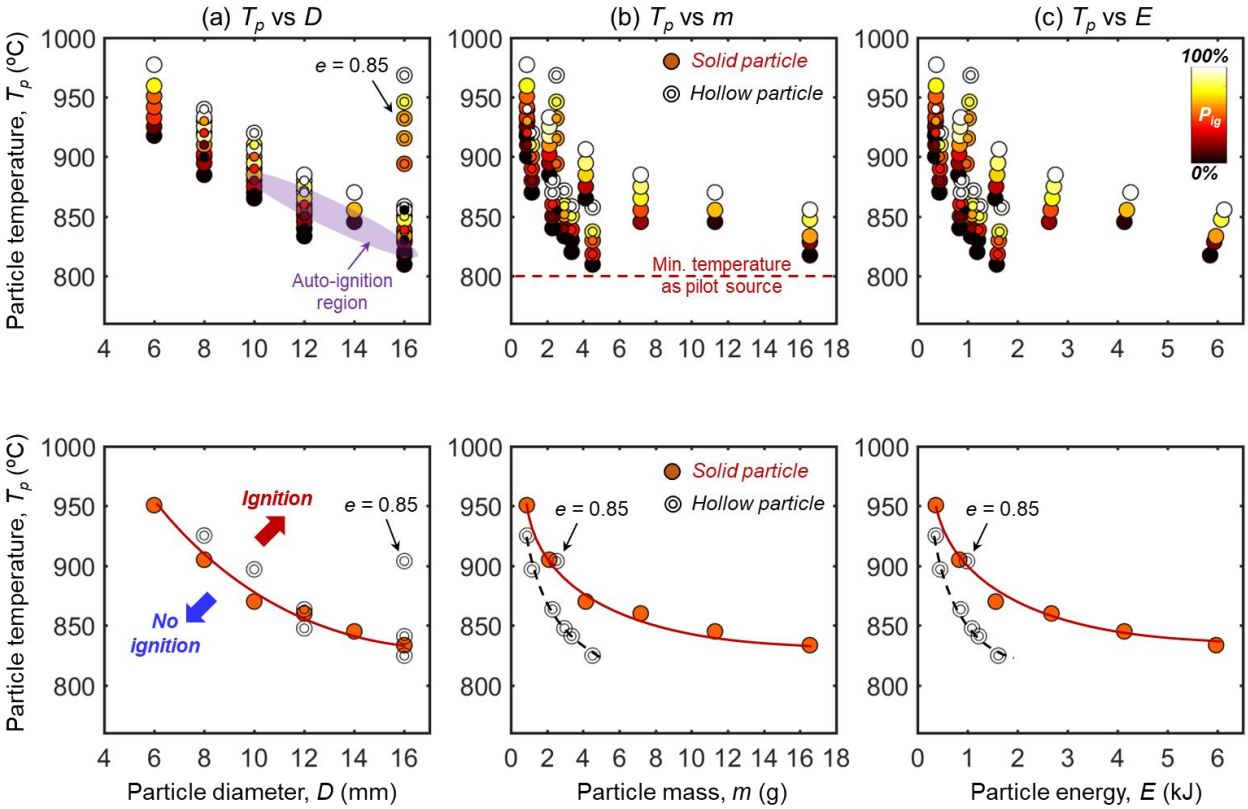

Fig. 4. Hot-particle temperature (T_p) and ignition probability (P_{ig}) vs. (a) particle diameter D, (b) particle mass m, and (c) effective energy E. The color bar scales the ignition probability from 0% (black) to 100% (white). The solid symbol presents the solid particle (including the previous data [13]), and the hollow symbol presents the hollow particle.

The void ratio (e) has little influence on the ignition limit unless it is larger than 0.80 (i.e., the particle shell is very thin). For example, to ignite the EPS sample with a 50% probability, the critical particle temperature needs to increase from 840 to 950 °C, as the particle diameter decreases from 16 to 6 mm. However, if the particle has a large void ratio of 0.85, the critical ignition temperature increases 50 °C, depending on the particle size and time scale of cooling and ignition (see more in Section 4).

Fig. 4b and c further present the influence of particle mass and energy on the ignition limit. The effective energy (E) of the particle, mainly affecting by the particle mass, is defined as

$$E = mc_p(T_p - T_a) = e\rho_s\left(\frac{\pi}{6}D^3\right)c_p(T_p - T_a) \quad (3)$$

where c_p is the specific heat of steel, and T_a is the ambient temperature. The minimum ignition

energy of the hot particle ranges from 0.3 kJ to 6.2 kJ. Clearly, neither the particle mass nor particle energy is **not** a good parameter to quantify the ignition limit. Specifically, for a given particle mass, the hollow particle can ignite the EPS foam with 50 °C lower than the solid particle. Similarly, the solid particle could require more than times the energy of the hollow particle to achieve the ignition.

These results are strongly against our common sense. Generally, we assume that the energy of the hot particle (or ignition source) is a characteristic parameter to determine the spotting ignition limit [13,22,23,27,37]. However, current experiments of moving hollow particles demonstrated that for the flaming ignition of EPS foam, the size and temperature of the particle (i.e., Fig. 4a) are the two best parameters to measure its spotting fire hazard, unless the void ratio is ≥ 0.85.

3.3. Effect of void ratio

To better quantify the influence of the void ratio, Fig. 5 shows the measured hot-particle ignition probability and the fitted ignition limit ($P_{ig} = 50\%$) as a function of the void ratio (e), initial temperature (T_p), and diameter (D). Because of the complex ignition process and large uncertainty, a possible ignition zone was found with a temperature range of 50 ºC for solid particles and >100 ºC for an extremely hollow particle (e = 0.85).

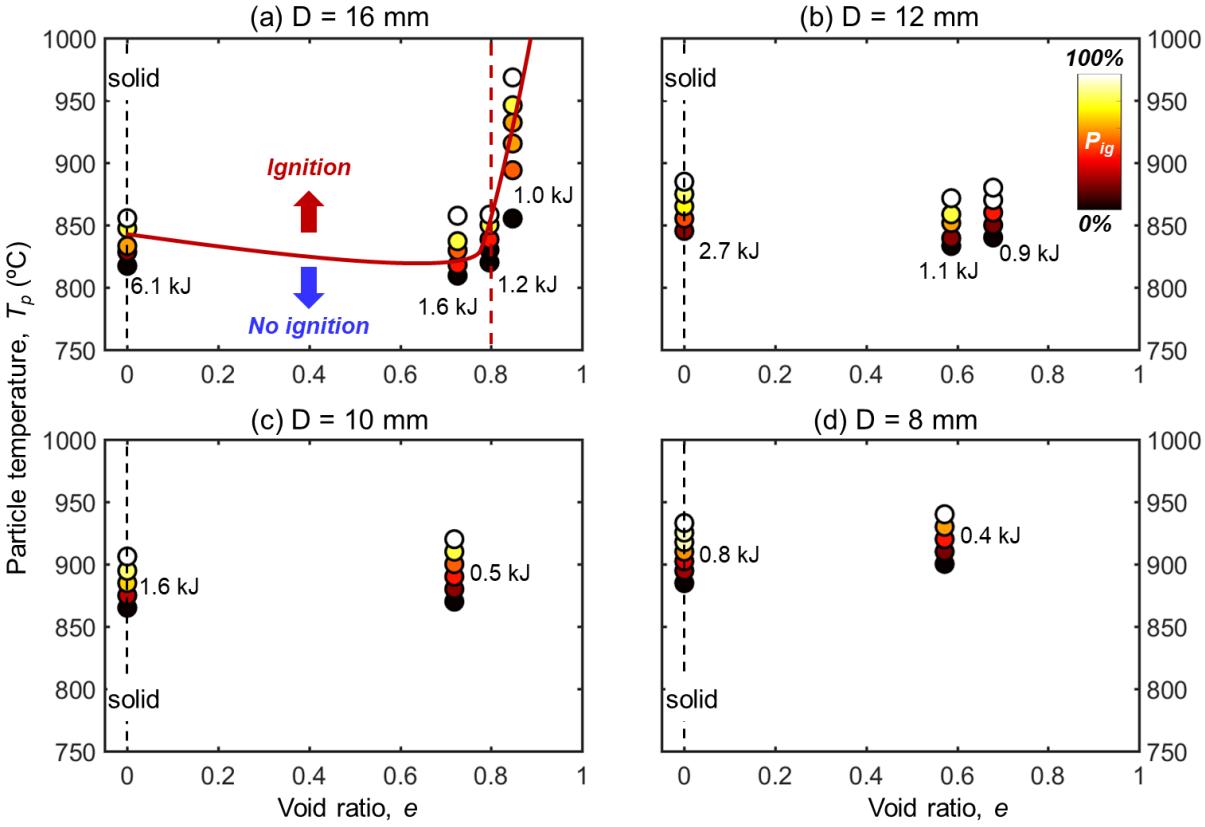

Fig. 5. Ignition probability for EPS foam as a function of the void ratio (e) and particle temperature (T_p) with the particle diameter of (a) 16 mm, (b) 12 mm, (c)10 mm, and (d) 8 mm, where a fitting curve is not provided if data points are limited.

Taking the 16-mm particle as an example (Fig. 5a), the critical particle temperature decreases slightly as the void ratio increases from 0 to 0.73, which is against the intuition. Moreover, as the void ratio increases, the critical particle temperature decreases from 6.1 kJ (e = 0) to 1.2 kJ (e = 0.8) and 1.0 kJ (e = 0.85). Similar behaviors are observed for other particle sizes in Fig. 5b-d. Therefore, we can conclude that given particle size,

(i) Critical particle energy for ignition cannot be defined if the particle is hollow; and

(ii) Larger particle energy does not necessarily mean a greater risk of hot-particle ignition or fire hazard.

Both are contrary to common sense or past research on solid particles. It is because, for hot-particle ignition of the low-density insulation foams, the interaction between the moving particles and the fuel is also important. For a hollow particle with a smaller bulk density, the embedding process is longer, which increases the effective heating time and the residence time of the particle.

On the other hand, if the particle is extremely hollow (e > 0.80 in Fig. 5a), the critical particle temperature increased significantly to 900 ºC, although its energy is minimum (1.0 kJ). Because of its small thermal inertia, this hollow particle will be quickly cooled below 800 ºC by both the fuel bed and the environment. Thus, for these hollow particles, both the particle energy and temperature, as well as the time scales of particle motion and diffusions, play important roles in the spotting ignition, as further discussed below.

3.4. Fire point, back boundary, and oxygen supply

As described above, the EPS foam can be briefly ignited by a hot particle (i.e., a flash), but with the sealed back boundary (Fig. 3a-b and Fig. 6a), the flame often cannot last to burn out the foam. In our previous work [13], it was found that to maintain a flame and burn out the fuel (i.e., the fire point) with the sealed back boundary, the particle temperature needs to further raise 100~200 ºC to above 1,100 ºC. Nevertheless, this fire point strongly depends on the back-boundary condition and the oxygen supply. Fig. 6 illustrated the influence of foam sample back boundaries, (a) sealed by the fireproof board, (b) held by metal mesh, and (c) no back cover, on the hot-particle (D = 16 mm, e = 0.73, T_p = 858 ºC) ignition phenomena. The original video recorded by the front-view camera can be found in Supplementary Videos S4-6. Note that the back-boundary condition of the fuel sample has no influence on the ignition limit (or flashpoint), because the ignition occurs on the top of the fuel, before the particle is cooled.

By using the semi-open mesh boundary (Fig. 6b), the hot particle 1st ignited the top surface of EPS foam with a flame. The flame extinguished within 2 s due to the lack of oxygen supply, similar to the case with the sealed back boundary in Fig. 6a. Then, there was a 2nd-stage hot-particle ignition inside the cavity, where after a few seconds, a flame was formed and stabilized that eventually burnt out the fuel bed. In other words, with the semi-open mesh boundary, as long as a flame can be initiated, it has a high probability of burning out the fuel. It is because there is a sufficient oxygen supply from the back

boundary to maintain the flame. The semi-open mesh boundary also allows the dripping of molten EPS with flame, which can further expand the fire hazard [41].

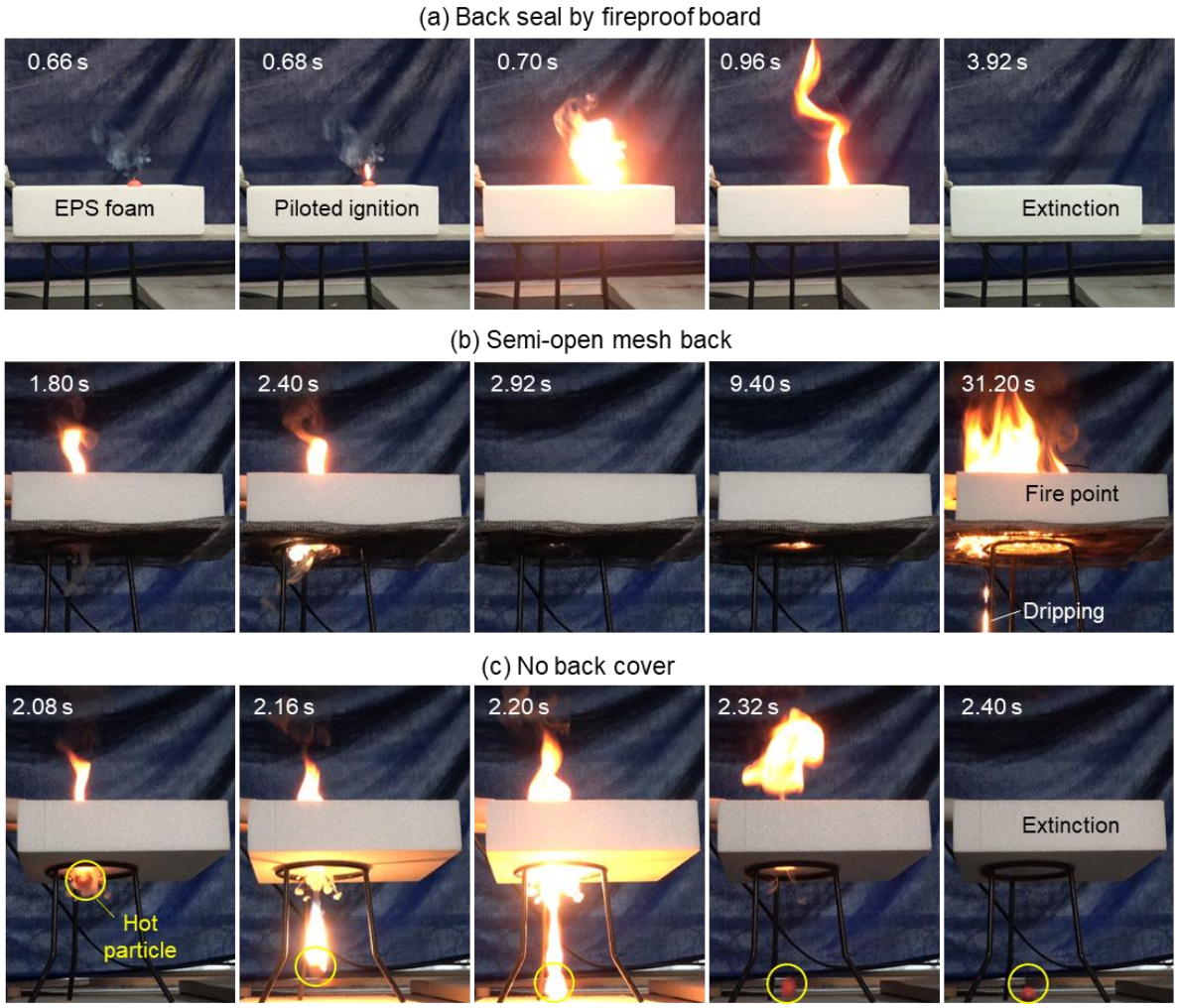

Fig. 6. The hot-particle ignition and burning processes of EPS foam with three back boundaries, (a) sealed fireproof board (Video S4), (b) semi-open metal mesh (Video S5), and (c) no back cover (Video S6), where the hot particle parameters are the same (D = 16 mm, e = 0.73, T_p = 858 °C).

Nevertheless, sufficient oxygen supply is not a sufficient condition to reach the fire point. Fig. 6c shows that without the back cover, the hot particle quickly penetrated through the foam sample and formed a strong flame. Despite good oxygen supply, and the flame was also extinguished in 2 s, so the ignition did not reach the fire point. It is because the molten EPS cannot maintain the flame without extra heating from the hot particle. Therefore, both a sufficient oxygen supply and a longer hot-particle residence time are necessary to reach the fire point. By satisfying both necessary conditions, the foams with a semi-open back boundary have the biggest fire hazard.

4. Discussions

Previously, we found that the hot-particle ignition of EPS foam is fundamentally a piloted ignition process, where the hot particle acts as both the heating source and the piloted source like a flame [13].

Thus, such spotting ignition has two characteristics,

(1) As a pilot source, the initial temperature of hot particle needs to exceed 800 ºC; and

(2) The particle motion and the contact between the particle and the fuel surface play critical roles.

Both characteristics are different from the hot-particle ignition of wildland fuels [25–28] or the spotting ignition by reactive firebrands [11,14] that involve in the smoldering processes.

For the piloted ignition by the hot inert particle, one of the major findings in our previous work [13] is that the competition between the residence time of moving particle (t_r) and the mixing time of the high-temperature pyrolysis gas and air (t_{mix}) that controls the ignition limit as

$$t_{ig} = t_{py} + t_{mix} + t_{chem} \approx t_{mix} \leq t_r \qquad (4a)$$

where the influence of gas-phase chemical time and chemical time can be ignored, because the small flame was found attached to the hot moving particle (T_p > 800 ºC) and before embedded, although it may not be sustained to ignite the whole EPS foam.

There is also strong evidence that sufficient fuel is pyrolyzed within a negligible time.

1) The particle temperature (>800 °C) is much higher than the characteristic pyrolysis temperature of EPS (lower than 350 °C from TGA), which can be quickly reached by the direct contact between hot particle and foam.
2) The particle energy is much larger than pyrolysis energy to reach the lower flammability limit of the pyrolysate.
3) The small flame was observed during the particle's rolling and embedding processes.
4) The critical particle temperature for ignition is independence of the foam density.

Thus, the mixing time for the hot moving particle controls the observed spotting ignition limits, rather than other time scales. Nevertheless, to fully explain the piloted ignition by hollow or porous particles, as well as the new auto-ignition phenomenon, an improved analysis with more time scales should be considered.

4.1. Piloted ignition and time-scale analysis

For the piloted ignition by a hot particle on the fuel top surface, the mixing time can be estimated as the fuel-gas diffusion time across the boundary layer on the particle [16] as

$$t_{mix} \sim \frac{\delta^2}{\alpha} \approx \frac{(D/Nu_D)^2}{\alpha} \qquad \text{(piloted ignition)} \qquad (5a)$$

where the diffusivity (α) increases with the temperature. Thus, the mixing time decreases as the particle temperature increases, as illustrated in Fig. 7a.

For a moving particle, the longer residence time occurs, when it just stops rolling on the top surface

while not fully embedding into the foam. The residence time may be estimated as

$$t_r \approx \sqrt{\frac{2D}{a}} \tag{6}$$

The local acceleration (a) is controlled by the gravity force of particle (mg) and the resistance tension force of foam (τA) as

$$a \approx \frac{mg - \tau A}{m} = g - \frac{3}{2}\frac{\tau}{\rho_s}\frac{1}{D(1-e)} \tag{7}$$

where the resistance tension (τ) decreases as the particle temperature increases, and A is the contact area between particle and foam, which changes during the embedding process. Thus, the residence time increases as the void ratio (e) increases, and it also decreases as the particle temperature and size increase (see Fig. 7a).

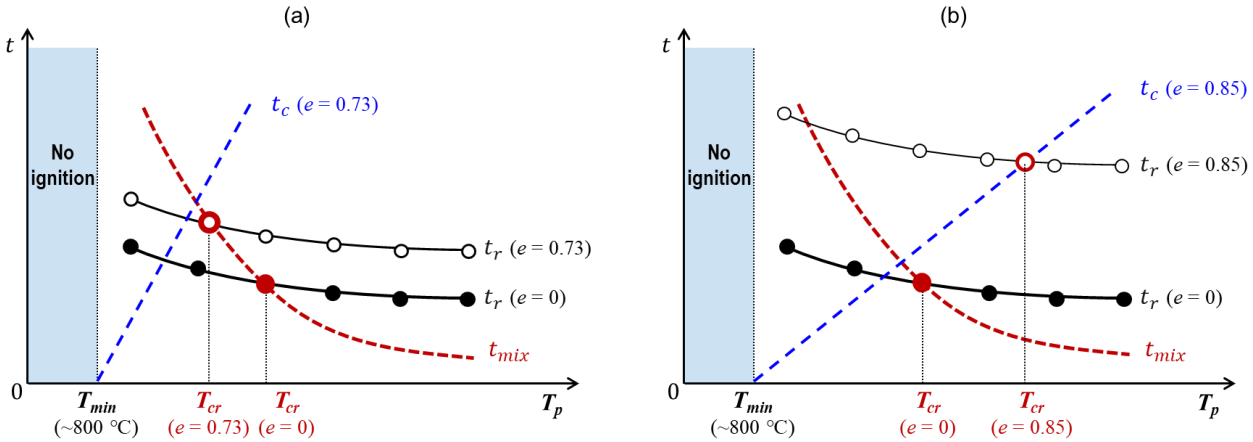

Fig. 7. The mixing time (t_{mix}), embedding residence time (t_r), and cooling time (t_c) versus the particle temperature (T_p), (a) particles with a small void ratio, and (b) the extremely hollow particle (large void ratio), where time zero is the moment that the particle stops.

This residence time of embedding can be measured in the experiment by the frame-by-frame video processing. For example, for a 16-mm solid particle, t_r decreases with increasing particle temperature, that is, 2,750 ± 20 ms (300 ºC), 570 ± 20 ms (600 ºC), 280 ± 10 ms (817 ºC), 250 ± 10 ms (830 ºC), and 220 ± 10 ms (847 ºC). Moreover, the influence of the void ratio on residence time can be quantified as well. For example, for a 16-mm solid particle with an initial temperature of 830 ºC, the residence time was measured to be 250 ± 10 ms (e = 0), 400 ± 10 ms (e = 0.73), 450 ± 10 ms (e = 0.80), and 540 ± 20 ms (e = 0.85), respectively. Therefore, as illustrated in Fig. 7a, the critical temperature for hollow particles could be slightly smaller than the solid particle, because the decrease of bulk density increases the residence time for piloted ignition. This explains the trend of critical particle temperature for small void ratios in Fig. 5.

4.2. Extremely hollow particle and cooling time

To further explain the critical temperature of hollow particles with extremely large avoid ratio (or highly porous particles), another necessary condition should be considered. That is, the particle cannot be cooled below the minimum temperature of piloting (about 800 ºC) before fully embedded into the fuel bed. In other words, the characteristic cooling time of hot particle (t_c) should be longer than its characteristic residence time on the fuel as

$$t_r \leq t_c \tag{4b}$$

Once exceeding the cooling time, the hot particle is no longer hot enough to be a pilot source.

Considering that the hot particle is cooled from its initial temperature (T_p) to the minimum pilot temperature ($T_{min} \approx 800$ ℃), the cooling process can be estimated as

$$\rho V c_p (T_p - T_{min}) \approx S h_c t_c \tag{8}$$

where c_p is the specific heat of the particle, $S = \pi D^2$ is the particle surface area, and h_c is the overall heat transfer coefficient for the cooling by the fuel bed and the environment, which counts both convective and radiant heat losses. Then, the cooling time (or the effective pilot time) of the particle is

$$t_c \approx \frac{\rho_s c_p}{6 h_c} (T_p - T_{min})(1 - e) D \tag{9}$$

which increases with the particle size and temperature, as illustrated and compared in Fig. 7a and b.

For solid particle and hollow particles of a small void ratio (Fig. 7a), the characteristic cooling time is much longer than the residence time, so it has a negligible influence on the piloted ignition. Nevertheless, for a very large void ratio (or extremely hollow particle), the particle needs to have a much higher temperature (Fig. 7b) to compensate for the fast cooling and maintain the minimum pilot temperature. This further explains the increasing trend of the critical particle temperature for large void ratios in Fig. 5.

Note that for a longer transport distance, the particle cooling process will be more important. Also, as the particle diameter decreases, the convective cooling coefficient increases significantly as $h \propto 1/D$. Thus, the smaller particle has a much shorter cooling time and a lower fire hazard.

4.3. Auto-ignition mechanism

As discovered in this work (Fig. 3b and Video S2), a 2nd-stage auto-ignition occurs after the 1st-stage flaming is smothered, and the particle is embedded into the foam bed. With a sealed back boundary, the particle cannot further pilot the flame without oxygen, although it is still sufficiently hot to decompose EPS foam and produce a large amount of pyrolysis gases. Driven by the buoyancy force, the pyrolysis gas floats upward and mixes with air, which is seen as a smoke plume (Fig. 3b). During the quick mixing process, if the mixture plume is still hot enough before floating above the flammable zone, the auto-ignition can occur. In other words, the necessary condition for the auto-ignition is that

the plume mixing time should be shorter than the cooling time as

$$t_{mix} \leq t_c \tag{10}$$

Note that the residence time of particle and the diffusion time of oxygen into the EPS sample are less important, because the auto-ignition occurs in the plume above the fuel bed (see 520 ms in Fig. 3b).

For such an auto-ignition, the mixing time of the pyrolysis gas and air could be estimated as

$$t_{mix} \approx \frac{\delta^2}{\alpha} \approx \frac{D^2}{\alpha} \qquad \text{(auto-ignition)} \qquad (5b)$$

where the characteristic size is the diameter of the particle (approximately the diameter of the vertical cavity), because the mixing occurs at the outlet of the cavity. Similar to Eq. 5a, as the particle temperature increases, the plume temperature increases, and the mixing time decreases (see Fig. 8).

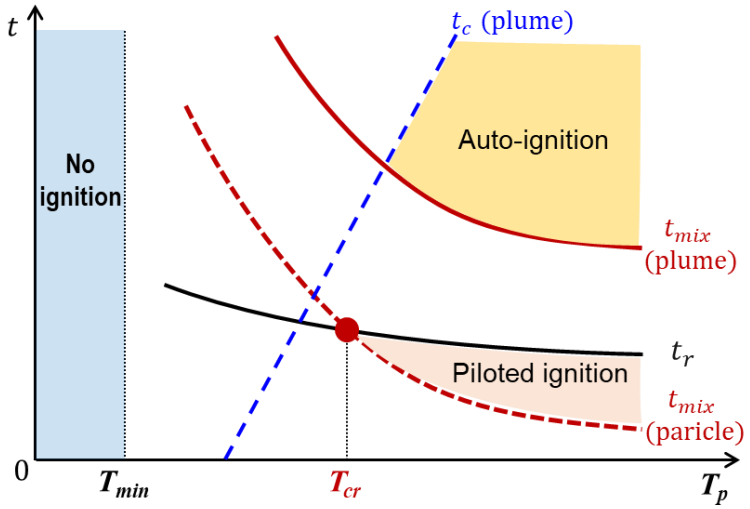

Fig. 8. Illustration of the piloted-ignition and auto-ignition regions as a function of particle temperature.

The characteristic cooling time of the plume also increases with the particle temperature (Fig. 8), which is similar to the cooling time of the particle in Fig. 7. Thus, if the particle is hot enough, the 2nd-stage auto-ignition may occur, and the ignition region is illustrated in Fig. 8. Note that the 2nd-stage auto-ignition process is more complex and random than the 1st-stage piloted ignition. Many other parameters, such as the thickness of the fuel sample and environment airflow, can affect the propensity of auto-ignition, which requires further research.

5. Conclusions

This work investigates the spotting ignition of a moving hot hollow metal particle, which is different from previous studies with a metal particle that is solid and static. The hot hollow steel particle with changing the void ratio, temperature, and diameter was dropped onto the expandable polystyrene (EPS) foam of 16 kg/m^3 with the influence of foam sample back boundaries, (a) sealed by the fireproof board, (b) held by metal mesh, and (b) no back cover. Results show that a smaller porous particle requires a much higher temperature for spotting ignition, following the hyperbolic relationship, and larger hot

particles generally pose a greater fire risk. Moreover, the minimum ignition temperature of hollow particles is close to solid particles (about 800 ℃), and the temperature and size of particle are better measures of the spotting fire risk than the mass and energy of particle.

As the void ratio increases, the minimum particle temperature for ignition first slightly decreases because the residence time of the moving particle increases. For extremely hollow particles, ignition requires a much higher particle temperature to overcome the fast cooling. Besides the piloted ignition by hot particle, the auto-ignition phenomenon is observed for the first time. The auto-ignition is controlled by the time scales of mixing around the moving particle and cooling of the fuel plume. Moreover, the semi-open fuel back boundary shows the biggest fire hazard, because both good oxygen supply and long particle residence time promote the ignition to the fire point and fuel burnout. This study deepens the understanding of the complex interaction between hot porous particles and foam materials in the spotting ignition process of the building façade.

Acknowledgments

This work is supported by the National Natural Science Foundation of China (No. 51706095, 51876183), Natural Science Foundation of Jiangsu Province (BK20171001), China Postdoctoral Science Foundation (2017M611798), and the Open Fund of SKLFS (HZ2017-KF09, HZ2019-KF02).

CRediT author statement

Supan Wang: Investigation, Methodology, Writing - Original Draft, Formal analysis; Funding acquisition. **Yu Zhang:** Investigation, Writing - Original Draft, Formal analysis. **Xinyan Huang:** Conceptualization, Methodology, Formal analysis; Supervision, Writing - Review & Editing.

References

[1] A.M. Papadopoulos, State of the art in thermal insulation materials and aims for future developments, Energy Build. (2005). doi:10.1016/j.enbuild.2004.05.006.

[2] M.S. McLaggan, J.P. Hidalgo, J. Carrascal, M.T. Heitzmann, A.F. Osorio, J.L. Torero, Flammability trends for a comprehensive array of cladding materials, Fire Saf J. (2020). doi:10.1016/j.firesaf.2020.103133.

[3] J. Schulz, D. Kent, T. Crimi, J.L.D. Glockling, T.R. Hull, A Critical Appraisal of the UK's Regulatory Regime for Combustible Façades, Fire Technol. (2020). doi:10.1007/s10694-020-00993-z.

[4] M. Bonner, G. Rein, Flammability and multi-objective performance of building façades: Towards optimum design, Int J High-Rise Build. 7 (2018) 363–374. doi:10.21022/IJHRB.2018.7.4.363.

[5] E. Guillaume, V. Dréan, B. Girardin, F. Benameur, T. Fateh, Reconstruction of Grenfell Tower fire. Part 1: Lessons from observations and determination of work hypotheses, Fire Mater. (2020). doi:10.1002/fam.2766.

[6] E. Ronchi, D. Nilsson, Fire evacuation in high-rise buildings: a review of human behaviour and modelling research, Fire Sci Rev. 2 (2013) 1–21. doi:10.1186/2193-0414-2-7.

[7] C.J. Rallis, B.M. Mangaya, Ignition of veld grass by hot aluminium particles ejected from clashing overhead transmission lines, Fire Technol. 38 (2002) 81–92. doi:10.1023/A:1013484932749.

[8] Y. Liu, J.L. Urban, C. Xu, C. Fernandez-Pello, Temperature and Motion Tracking of Metal Spark Sprays, Fire Technol. 55 (2019) 2143–2169. doi:10.1007/s10694-019-00847-3.

[9] L. Peng, Z. Ni, X. Huang, Review on the fire safety of exterior wall claddings in high-rise buildings in China, Procedia Eng. 62 (2013) 663–670. doi:10.1016/j.proeng.2013.08.112.

[10] J. Sun, L. Hu, Y. Zhang, A review on research of fire dynamics in high-rise buildings, Theor Appl Mech Lett. 3 (2013) 042001. doi:10.1063/2.1304201.

[11] S.L. Manzello, S. Suzuki, M.J. Gollner, A.C. Fernandez-Pello, Role of firebrand combustion in large outdoor fire spread, Prog Energy Combust Sci. 76 (2020) 100801. doi:10.1016/j.pecs.2019.100801.

[12] J. Song, S. Wang, H. Chen, Safety distance for preventing hot particle ignition of building insulation materials, Theor Appl Mech Lett. 4 (2014) 034005. doi:10.1063/2.1403405.

[13] S. Wang, X. Huang, H. Chen, N. Liu, G. Rein, Ignition of low-density expandable polystyrene foam by a hot particle, Combust Flame. 162 (2015) 4112–4118. doi:10.1016/j.combustflame.2015.08.017.

[14] A.F.-P.-F.S. Journal, undefined 2017, Wildland fire spot ignition by sparks and firebrands, Elsevier. (n.d.).

[15] A.C. Fernandez-Pello, Wildland fire spot ignition by sparks and firebrands, Fire Saf J. 91 (2017) 2–10. doi:10.1016/j.firesaf.2017.04.040.

[16] J. Quintiere, Fundamentals of Fire Phenomena, John Wiley & Sons, Ltd, London, 2006. doi:10.1002/0470091150.

[17] S.E. Caton, R.S.P. Hakes, M.J. Gollner, Review of Pathways for Building Fire Spread in the Wildland Urban Interface Part I : Exposure Conditions, Fire Technol. 53 (2017) 429–473. doi:10.1007/s10694-016-0589-z.

[18] R.S.P. Hakes, S.E. Caton, D.J. Gorham, M.J. Gollner, A Review of Pathways for Building Fire Spread in the Wildland Urban Interface Part II: Response of Components and Systems and Mitigation Strategies in the United States, Fire Technol. 53 (2017) 475–515. doi:10.1007/s10694-016-0601-7.

[19] W. Fang, Z. Peng, H. Chen, Ignition of pine needle fuel bed by the coupled effects of a hot metal particle and thermal radiation, Proc Combust Inst. (2020). doi:10.1016/j.proci.2020.05.032.

[20] C. Lautenberger, C. Fernandez-Pello, A model for the oxidative pyrolysis of wood, Combust Flame. 156 (2009) 1503–1513. doi:10.1016/j.combustflame.2009.04.001.

[21] G. Rein, Smoldering Combustion, SFPE Handb Fire Prot Eng. 2014 (2014) 581–603. doi:10.1007/978-1-4939-2565-0_19.

[22] J.L. Urban, C.D. Zak, J. Song, C. Fernandez-Pello, Smoldering spot ignition of natural fuels by a hot metal particle, Proc Combust Inst. 36 (2017) 3211–3218. doi:10.1016/j.proci.2016.09.014.

[23] J.L. Urban, C.D. Zak, C. Fernandez-Pello, Cellulose spot fire ignition by hot metal particles, Proc Combust Inst. 35 (2015) 2707–2714. doi:10.1016/j.proci.2014.05.081.

[24] P. Yin, N. Liu, H. Chen, J.S. Lozano, Y. Shan, New Correlation Between Ignition Time and Moisture Content for Pine Needles Attacked by Firebrands, Fire Technol. 50 (2014) 79–91.

doi:10.1007/s10694-012-0272-y.

[25] R.M. Hadden, S. Scott, C. Lautenberger, C.C. Fernandez-Pello, Ignition of Combustible Fuel Beds by Hot Particles: An Experimental and Theoretical Study, Fire Technol. 47 (2011) 341–355. doi:10.1007/s10694-010-0181-x.

[26] J.L. Urban, C.D. Zak, C. Fernandez-Pello, Spot Fire Ignition of Natural Fuels by Hot Aluminum Particles, Fire Technol. 54 (2018) 797–808. doi:10.1007/s10694-018-0712-4.

[27] S. Wang, X. Huang, H. Chen, N. Liu, Interaction between flaming and smouldering in hot-particle ignition of forest fuels and effects of moisture and wind, Int J Wildl Fire. 26 (2017) 71–81. doi:10.1071/WF16096.

[28] P.F.M. Ellis, Fuelbed ignition potential and bark morphology explain the notoriety of the eucalypt messmate "stringybark" for intense spotting, Int J Wildl Fire. 20 (2011) 897–907. doi:10.1071/WF10052.

[29] J. Song, X. Huang, N. Liu, H. Li, L. Zhang, The Wind Effect on the Transport and Burning of Firebrands, Fire Technol. 53 (2017) 1555–1568. doi:10.1007/s10694-017-0647-1.

[30] D.X. Viegas, M. Almeida, J. Raposo, R. Oliveira, C.X. Viegas, Ignition of Mediterranean Fuel Beds by Several Types of Firebrands, Fire Technol. 50 (2014) 61–77. doi:10.1007/s10694-012-0267-8.

[31] S.L. Manzello, T.G. Cleary, J.R. Shields, A. Maranghides, W. Mell, J.C. Yang, Experimental investigation of firebrands: Generation and ignition of fuel beds, Fire Saf J. 43 (2008) 226–233. doi:10.1016/j.firesaf.2006.06.010.

[32] S.L. Manzello, S.-H. Park, T.G. Cleary, Investigation on the ability of glowing firebrands deposited within crevices to ignite common building materials, Fire Saf J. 44 (2009) 894–900. doi:10.1016/j.firesaf.2009.05.001.

[33] S.L. Manzello, Y. Hayashi, T. Yoneki, Y. Yamamoto, Quantifying the vulnerabilities of ceramic tile roofing assemblies to ignition during a firebrand attack, Fire Saf J. 45 (2010) 35–43.

[34] S. Suzuki, E. Johnsson, A. Maranghides, S.L. Manzello, Ignition of Wood Fencing Assemblies Exposed to Continuous Wind-Driven Firebrand Showers, Fire Technol. 52 (2016) 1051–1067.

[35] P.F.M. Ellis, The likelihood of ignition of dry-eucalypt forest litter by firebrands, Int J Wildl Fire. 24 (2015) 225–235. doi:10.1071/WF14048.

[36] A. Ganteaume, C. Lampin-Maillet, M. Guijarro, C. Hernando, M. Jappiot, T. Fonturbel, P. Ṕrez-Gorostiaga, J.A. Vega, Spot fires: Fuel bed flammability and capability of firebrands to ignite fuel beds, Int J Wildl Fire. 18 (2009) 951–969. doi:10.1071/WF07111.

[37] S. Wang, H. Chen, N. Liu, Ignition of Expandable Polystyrene Foam by a Hot Particle : An Experimental and Numerical Study, J Hazard Mater. 283 (2015) 536–543. doi:10.1016/j.jhazmat.2014.09.033.

[38] D. Drysdale, An Introduction to Fire Dynamics, 3rd ed., John Wiley & Sons, Ltd, Chichester, UK, 2011. doi:10.1002/9781119975465.

[39] S. Suzuki, S.L. Manzello, Role of accumulation for ignition of fuel beds by firebrands, Appl Energy Combust Sci. 1–4 (2020) 100002. doi:10.1016/j.jaecs.2020.100002.

[40] Z. Tao, B. Bathras, B. Kwon, B. Biallas, M.J. Gollner, R. Yang, Effect of firebrand size and geometry on heating from a smoldering pile under wind, Fire Saf J. (2021) 103031. doi:10.1016/j.firesaf.2020.103031.

[41] P. Sun, S. Lin, X. Huang, Ignition of thin fuel by thermoplastic drips: An experimental study for the dripping ignition theory, Fire Saf J. 115 (2020) 103006. doi:10.1016/j.firesaf.2020.103006.

Appendix

The raw EPS sample was ground into particles to subject the dynamic thermal decomposition experiments. The thermal analysis was conducted with a TA Instruments SDT-Q600 simultaneous analyzer, to record the TG / DSC curves of the EPS foam at a heating rate of 10 K min^{-1} under both air and nitrogen atmospheres. The initial mass of sample was about 3 mg. Experiments were repeated twice for each experimental condition, and good repeatability is shown. Fig. A1 shows the mass-loss rate and heat flow curves of the EPS foam. Regardless of the oxygen concentration, the mass loss rate rapidly increases at 250 ℃, which can be defined as the pyrolysis temperature (T_{py}). The exothermic heat (ΔH) of EPS foam can be calculated by integrating the heat flow curve and is 5.2 MJ kg^{-1} and 33.8 MJ kg^{-1} for two reaction stages.

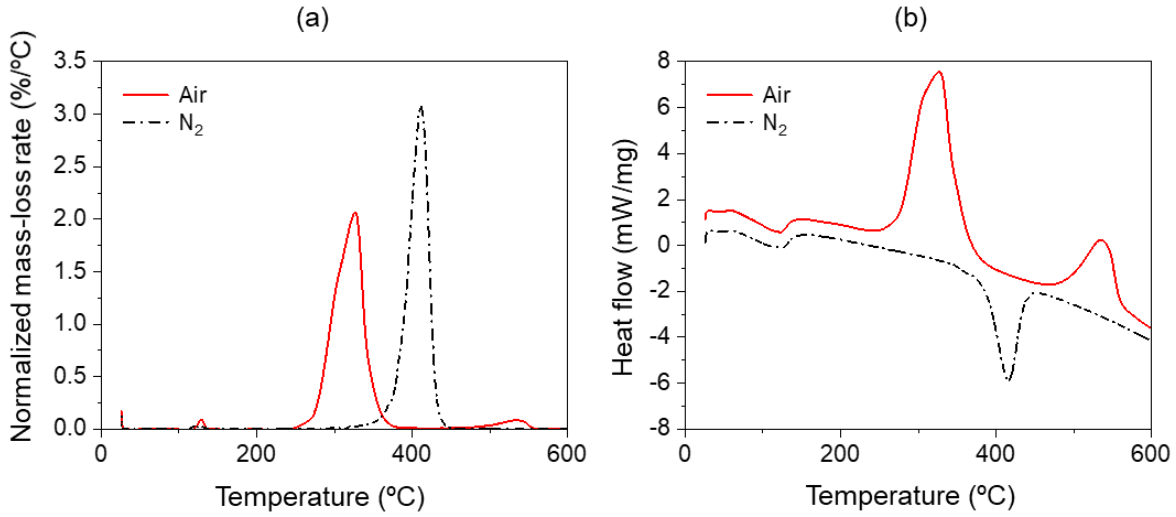

Fig. A1. TGA-DSC results of EPS foam under air and nitrogen flow at a heating rate of 10 K min^{-1}, (a) normalized mass loss rate and (b) heat flow as a function of temperature where DTG is the differentiated TG or the mass loss rate.